CCS CHINESE CHEMICAL SOCIETY

ROYAL SOCIETY OF CHEMISTRY

RESEARCH ARTICLE

Check for updates

Constructing [Co$_6^{II}$] hexagon-centered heterometallic {Ln$_6$Co$_6$} (Ln = Y, Eu and Dy) clusters with a calix[8]arene ligand†

Haitao Han,‡[a,b] You-Song Ding, ‡[c] Xiaofei Zhu,[a] Tian Han,[c] Yan-Zhen Zheng *[c] and Wuping Liao *[a]

Three isostructural 3d–4f polynuclear clusters {(Ln$_6^{III}$Co$_6^{II}$)(C8A)$_3$} (Ln = Y (**CIAC-248**), Eu (**CIAC-249**), Dy (**CIAC-250**); C8A = *p-tert*-butylcalix[8]arene) were synthesized under solvothermal conditions. These three compounds feature some tripod-like entities in which three Ln$_2$-C8A secondary building units acting as the legs bolster a [Co$_6$] hexagon. Magnetic study indicated that the complex {(Eu$_6^{III}$Co$_6^{II}$)(C8A)$_3$} (**CIAC-249**) exhibits spin glass behaviour at ≈9 K, and the complex {(Dy$_6^{III}$Co$_6^{II}$)(C8A)$_3$} (**CIAC-250**) shows slow relaxation of magnetization.

Introduction

Heterometallic 3d–4f clusters have attracted considerable attention due to their fascinating structures, interesting magnetic properties such as single-molecule magnet (SMM) behaviour, and potential applications in high-density information storage and quantum computing.[1–3] Commonly, the syntheses of these types of clusters are based on some shielded or multidentate ligands which can act as the magnetic coupling mediator. Calixarenes have been proven to be excellent multidentate ligands to construct single-molecule magnets due to their polyphenolic nature, which can not only induce ferromagnetic or antiferromagnetic coupling efficiently but also assume diverse coordination modes. To date, there have been some reports on the construction of paramagnetic molecular clusters with calixarenes. For example, Dalgarno and Brechin[4–7] applied methylene-bridged calix[4]arene in the construction of SMMs and magnetic coolers. We[8,9] and others[10–13] used thia- and sulfonyl-bridged calix[4]arenes for the preparation of polynuclear clusters possessing interesting magnetic

properties. However, to the best of our knowledge, polynuclear clusters based on larger calixarenes such as *p-tert*-butylcalix[8] arene with SMM properties and ferromagnetic ordering behaviours are rare.[14–16] Compared to calix[4]arene, calix[8]arene, which has more coordination sites, variable conformation and higher flexibility, may generate novel materials with interesting properties.[17,18] In addition, a carbonate anion is also a good bridge due to its various bridging modes, such as μ$_2$-CO$_3^{2-}$,[19,20] μ$_3$-CO$_3^{2-}$,[21,22] μ$_4$-CO$_3^{2-}$,[23,24] and μ$_6$-CO$_3^{2-}$.[25–27] Furthermore, we found that calix[8]arene adopting a double cone conformation can form a Ln$_2$-C8A secondary building unit (SBU) when reacting with lanthanide ions and the Ln$_2$-C8A SBUs can bond some transition metals (TM) to form heterometallic 3d–4f clusters. Here, we present the crystal structures and magnetic properties of three {(Ln$_6^{III}$Co$_6^{II}$)(C8A)$_3$} compounds (Ln = Y (**CIAC-248**), Eu (**CIAC-249**), Dy (**CIAC-250**); C8A = *p-tert*-butylcalix[8]arene) incorporating a central μ$_6$-carbonate anion. These compounds exhibit ferromagnetic long-range ordering or SMM properties.

Experimental

Starting materials

All starting materials were of analytical reagent grade and used as received without further purification. *p-tert*-Butylcalix[8] arene was prepared according to the literature method.[28]

Syntheses of compounds CIAC-248–250

{[(Y$_6$Co$_6$)(C8A)$_3$(CH$_3$OH)$_5$(CH$_3$O$^-$)$_3$(CO$_3^{2-}$)(DMF)$_6$(CH$_3$COO$^-$)$_2$]}· 2.3H$_2$O 0.35CH$_3$OH·[(C$_2$H$_5$)$_3$NH$^+$] (**CIAC-248**). Blue block crystals were obtained by the solvothermal reaction of a mixture of

[a]*State Key Laboratory of Rare Earth Resource Utilization, Changchun Institute of Applied Chemistry, Chinese Academy of Sciences, Changchun 130022, China. E-mail: wpliao@ciac.ac.cn; Fax: +86(431)85698041*
[b]*University of Chinese Academy of Sciences, Beijing 100049, China*
[c]*Frontier Institute of Science and Technology (FIST), State Key Laboratory of Mechanical Behavior of Materials and MOE Key Laboratory for Nonequilibrium Synthesis and Modulation of Condensed Matter, Xi'an Jiaotong University, Xi'an 710054, China. E-mail: zheng.yanzhen@xjtu.edu.cn*
†Electronic supplementary information (ESI) available: Additional figures, UV-vis spectra, TG/DSC curves and FT-IR spectra. CCDC 2013506–2013508. For ESI and crystallographic data in CIF or other electronic format, see DOI: 10.1039/d0qi00792g
‡These authors contributed equally.

4070 | *Inorg. Chem. Front.*, 2020, **7**, 4070–4076

This journal is © the Partner Organisations 2020

C8A (0.065 g, 0.04 mmol), $Co(CH_3COO)_2 \cdot 4H_2O$ (0.038 g, 0.15 mmol), $Y(CH_3COO)_3 \cdot 6H_2O$ (0.04 g, 0.39 mmol), CH_3OH (6 mL), triethylamine (1.1 mL) and several drops of DMF in a 20 mL Teflon-lined autoclave which was kept at 150 °C for 3 days and then slowly cooled to room temperature at about 4 °C h^{-1}. The crystals were isolated by filtration and washed with methanol and dried under air. Yield: 36% with respect to Y. Elemental analysis (%): calcd for $[C_{292}H_{390}Y_6Co_6N_6O_{45}]$ (excluding disordered solvent molecules): C, 62.73; N, 1.50; H, 6.98. Found: C, 62.23; N, 1.31; H, 6.31. FT-IR (KBr pellet, cm^{-1}): 3527(w), 2955(s), 1650(s), 1569(w), 1454(s), 1387(m), 1360(m), 1293(s), 1212(s), 1125(w), 1044(m), 909(w), 875(w), 822(m), 754(m), 674(w).

$\{[(Eu_6Co_6)(C8A)_3(CH_3OH)_5(CH_3O^-)_3(CO_3{}^{2-})$ $(DMF)_6(CH_3COO^-)_2]\} \cdot 2H_2O \cdot [(C_2H_5)_3NH^+]$ (**CIAC-249**). The procedure was similar to the synthesis of **CIAC-249** except that $Y(CH_3COO)_3 \cdot 6H_2O$ was substituted with $Eu(CH_3COO)_3 \cdot 6H_2O$. The crystals were isolated as blue block crystals in 32% yield based on Eu. Elemental analysis (%): calcd $[C_{292}H_{390}Eu_6Co_6N_6O_{45}]$ (excluding disordered solvent molecules): C, 58.76; N, 1.41; H, 6.54. Found: C, 58.49; N, 1.32; H, 6.65. FT-IR (KBr pellet, cm^{-1}): 3528(w), 2953(s), 1656(s), 1466(s), 1396(m), 1358(m), 1293(s), 1207(s), 1125(w), 1027(m), 908(w), 876(w), 821(m), 745(m), 685(w).

$\{[(Dy_6Co_6)(C8A)_3(CH_3OH)_5(CH_3O^-)_3(CO_3{}^{2-})$ $(DMF)_6(CH_3COO^-)_2]\} \cdot 3H_2O \cdot CH_3OH \cdot [(C_2H_5)_3NH^+]$ (**CIAC-250**). The procedure was similar to the synthesis of **CIAC-248** except that $Y(CH_3COO)_3 \cdot 6H_2O$ was substituted by Dy$(CH_3COO)_3 \cdot 6H_2O$. The crystals were isolated as blue block crystals in 32% yield based on Dy. Elemental analysis (%): calcd for $[C_{292}H_{390}Dy_6Co_6N_6O_{45}]$ (excluding disordered solvent molecules): C, 58.14; N, 1.39; H, 6.49. Found: C, 58.02; N, 1.28; H, 6.39. FT-IR (KBr pellet, cm^{-1}): 3528(w), 2953(s), 1656(s), 1467(s), 1396(m), 1358(m), 1293(s), 1207(s), 1119(w), 1038(m), 914(w), 870(w), 815(m), 750(m), 674(w).

X-ray structure determination

The X-ray intensity data for compounds **CIAC-248–250** were collected on a Bruker D8 QUEST system with Cu Kα radiation ($\lambda = 0.15418$ nm) operated at 50 W (50 kV, 1 mA). The crystal structures were solved by means of direct methods and refined employing full-matrix least squares on F^2 (SHELXTL-97).[29] The large R_1 and wR_2 factors of compounds **CIAC-248–250** might be due to the weak high-angle diffractions and the disorder of *p-tert*-butyl groups. Hydrogen atoms of the organic ligands were generated theoretically onto the specific atoms and refined isotropically with fixed thermal factors. CCDC 2013506–2013508† contain the supplementary crystallographic data for this paper.

Physical measurements

Elemental analysis of C, N, and H was performed using a Vario EL instrument. TGA measurement was performed using a NETZSCH STA 449F3. FT-IR spectra were obtained with a Bruker Vertex 70 spectrometer. Magnetic susceptibility measurements were carried out with a Quantum Design MPMS-XL7 SQUID magnetometer. Freshly prepared crystalline samples were embedded in eicosane to avoid any field-induced crystal reorientation. Diamagnetic corrections were applied for eicosane and for the molecule, the latter being calculated from the Pascal constants. X-ray powder diffraction (XRD) measurements were performed on a D8 Focus diffractometer (Bruker) ranging from 0°–40° with Cu Kα radiation ($\lambda = 0.15418$ nm).

Results and discussion

Single-crystal X-ray diffraction analysis reveals that compounds **CIAC-248–250** are isostructural and feature a tripod-like unit composed of a wrapped $\{Co_6\}$ hexagon and three Ln$_2$-C8A SBUs (Fig. 1). So compound **CIAC-250** is described in detail as an example. Complex **CIAC-250** crystallizes in the monoclinic system with the space group $C2/c$. In the structure, three *p-tert*-butylcalix[8]arene molecules adopt the double cone conformation. Each conic subunit of the calix[8]arene molecule binds a Dy atom through its oxygen atoms at the lower rim so that a Dy$_2$-C8A secondary building unit (SBU) is formed, which is a common unit found in the compounds of 4f/5f metals and calix[8]arene. Six adjacent Co atoms are bonded to the same μ_6-$CO_3{}^{2-}$ anion *in situ* generated from the decomposition of DMF to form a $\{Co_6\}$ hexagonal plate. Furthermore, this hexagon is bolstered by three Dy$_2$-C8A SBUs to form a tripod-like $\{(Ln_6^{III}Co_6^{II})(C8A)_3\}$ entity (Fig. 2 and 3). It should be noted that all three calix[8]arene molecules in an isolated entity are nearly perpendicular to the planar $\{Co_6\}$ hexagon (Fig. S3†). The extended structure of compound **CIAC-250** is stacked by these dodecanuclear heterometallic units through supramolecular interactions (Fig. S4†).

For the $Ln_6^{III}Co_6^{II}$ core, there are twelve crystallographically independent metal sites which have three types of coordination. Each Co atom is five coordinated in a distorted trigonal bipyramid coordination geometry. The coordination geome-
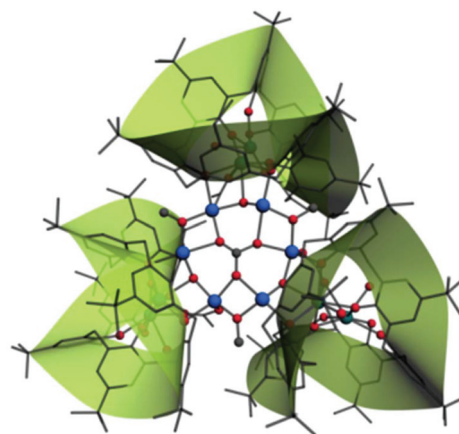

Fig. 1 Molecular structure of compound **CIAC-250**. Hydrogen atoms and solvent molecules are omitted for clarity. Blue: Co atoms; green: Dy atoms; red: O atoms; gray: C atoms.
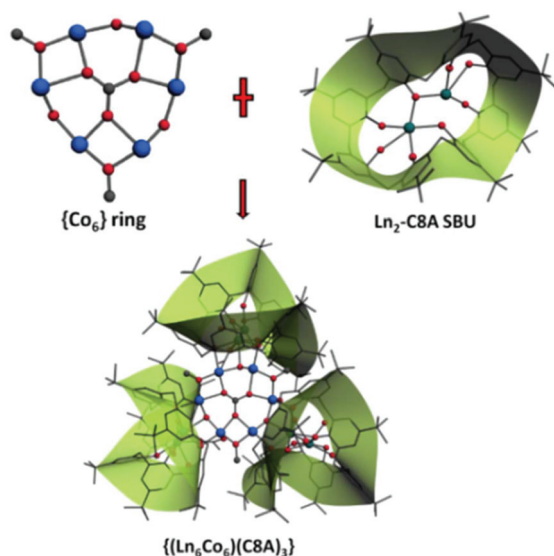
This journal is © the Partner Organisations 2020

Inorg. Chem. Front., 2020, **7**, 4070–4076 | **4071**

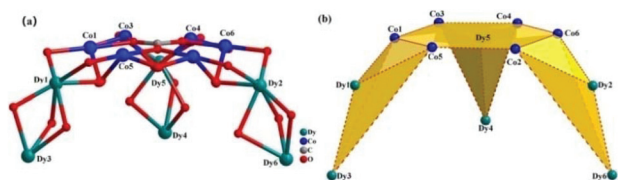Fig. 2 Scheme of the assembly of compound **CIAC-250**.

Fig. 3 Arrangement of the metal ions of compound **CIAC-250**.

tries of Dy(III) ions were calculated by SHAPE analysis (Table S2†).[30,31] Site Dy1 is seven coordinated in a capped octahedron with C_{3v} local symmetry. Sites Dy2, Dy4 and Dy5 are also seven coordinated, but in a capped trigonal prism with C_{2v} local symmetry. Sites Dy3 and Dy6 are eight coordinated in a biaugmented trigonal prism J50 with C_{2v} local symmetry. The distances of the Dy–O and Co–O bonds are in the range of 2.18–2.89 Å and 1.93–2.13 Å, respectively. The O–Dy–O and O–Co–O angles fall in the ranges of 52.7–159.7° and 74.8–178.6°. It is noted that the 3d–4f heterometallic compounds having a $\mu_6\text{-CO}_3^{2-}$ bridging-[Co$_6$] ring are documented for the first time.

Magnetic properties

The variable-temperature direct current (dc) magnetic susceptibility data for all compounds were collected under a 1 kOe applied field at the temperature range of 2–300 K (Fig. 4), and the field (H) dependence of the magnetizations (M) for these three complexes was measured up to 7 T at low temperatures (Fig. S6–S8†). The χT value for **CIAC-248** is 19.88 emu K mol^{-1} at room temperature, which is larger than the spin-only value (11.25 emu K mol^{-1}) expected for six uncoupled Co(II) ions ($S = 3/2$, $g = 2.0$), owing to the contribution from the orbital angular momentum. Upon cooling, the χT value decreases slowly and reaches 5.75 emu K mol^{-1} at 2 K, presumably corresponding to the depopulation of higher Kramers doublets
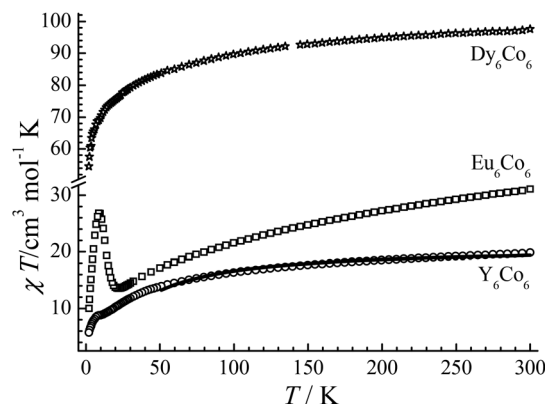

Fig. 4 The χT versus T plots for **CIAC-248, 249** and **250** under a 1 kOe dc field. The solid line is the best fit.

of the Co(II) centers and possible antiferromagnetic coupling between Co(II) ions. The magnetization for **CIAC-248** increases slowly with the field and reaches a maximum value of 6.30 μ_B at 2 K and 7 T.

For **CIAC-249**, although the Eu(III) ion ($J = 0$, $^7F_0$) possesses a diamagnetic ground state, the χT value at 300 K (31.10 emu K mol^{-1}) is much larger than that of **CIAC-248**. Such a large value is due to a certain amount of magnetic moment from the excited states (e.g., $^7F_1$) of the Eu(III) ion. The χT value is about 1.87 emu K mol^{-1} for each Eu ion at room temperature based on complex **CIAC-248**, which is close to the reported value.[32] The χT values decrease slowly as the temperature decreases to 12.56 emu K mol^{-1} at 22 K, followed by a sharp increase to a maximum value of 26.81 emu K mol^{-1} at 8.7 K, which indicates ferromagnetic interactions in the {Eu$_6$Co$_6$} cluster, and then drop to 10.03 emu K mol^{-1} at 2 K. The field dependence of magnetizations for **CIAC-249** gives a small value of 5.98 μ_B at 2 K and 7 T, which is close to those of **CIAC-248**, in accordance with the diamagnetic ground state of Eu(III) ions.

For **CIAC-250**, the χT value at room temperature (97.56 emu K mol^{-1}) is consistent with the expected value of six uncoupled Dy(III) ions ($S = 5/2$, $L = 5$, $g = 4/3$, $^6H_{15/2}$) and six isolated Co(II) ions. The χT value is smaller than the expected value with the orbital angular momentum from Co(II) ions, owing to the antiferromagnetic coupling between Dy(III) and Co(II). The χT values decrease gradually from 300 to 50 K and much rapidly below 50 K. At 2 K, the χT value is 54.55 emu K mol^{-1} and the maximum M value is 34.82 μ_B at 7 T. This unsaturation M value indicates the presence of magnetic anisotropy and/or low-lying excited states in the system. The program PHI was used to fit the magnetic susceptibility of **CIAC-248** with a minimal model (eqn (1)),[33] which can reproduce the temperature-dependent susceptibility at the temperature range from 50 K to 300 K (Fig. 4) and provide a reasonable estimate of the intramolecular magnetic exchange coupling (J) between the Co(II) ions. The best simulation gives $J = -3.15$ cm^{-1} with $g = 2.73$. Attempts for fitting the lower temperature data failed, probably due to the interplay and competition of spin-orbital

4072 | *Inorg. Chem. Front.*, 2020, **7**, 4070–4076

This journal is © the Partner Organisations 2020

coupling and magnetic interactions. The alternating current (ac) susceptibility measurement of **CIAC-248** at the frequency of 1488 Hz with a zero dc field displays a paramagnetic property (Fig. S9†), thus showing neither magnetic ordering nor slow relaxation of the magnetization above 2 K.

$$\hat{H} = -2J\left(\sum_{i=1}^{5} S_i S_{i+1} + S_6 S_1\right) + g\mu_B \sum_{i=1}^{6} S_i H \qquad (1)$$

As complex **CIAC-249** shows a peak at 8.7 K in its χT–T plots, further magnetic investigation was performed. The zero-field cooled (ZFC) and field-cooled (FC) magnetic susceptibility for **CIAC-249** was recorded under a field of 50 Oe. Both the peak of the ZFC curve and the divergence of the ZFC and FC curves appear at about 9.2 K (Fig. 5), indicating a transition from a paramagnetic state to either a long-range ordering, a spin-glass state or a superparamagnetic state.[34] Magnetic hysteresis measurements show a clear hysteresis loop at 2 K with a coercivity field of 580 Oe and a remnant magnetization of $0.38\mu_B$, and a closed hysteresis loop at 9 K, indicative of a magnet behaviour (inset in Fig. 5 and Fig. S13†).

Ac magnetic susceptibility measurements for **CIAC-249** were further carried out under a zero dc field. Wide peaks of the in-phase (χ') and out-of-phase (χ'') signals were observed between 8 K and 10 K with a very weak frequency dependence, supporting the existence of spin glassy behaviour (Fig. 6). The parameter $\varphi = (\Delta T_p/T_p)/(\Delta \log f)$ was estimated as 0.02, which falls into the range of a spin glass and excludes a superparamagnet.[35,36] We tried to fit the relaxation times at various temperatures via the Arrhenius law ($\tau = \tau_0 \exp(U_{eff}/k_B T)$, where τ_0 is a pre-exponential factor and U_{eff} is the energy barrier), and obtained ΔE = 1176 K and τ_0 = 2.43 × 10^{-57} s (Fig. S10†). This rather fast τ_0 also excludes the possibility of an SMM. Those behaviours are similar to other Co clusters with spin glass behaviours.[37,38] For **CIAC-249**, the spin glassy behavior probably is attributed to the weak magnetic moment from Eu(III) ions that modified the magnetic coupling between Co(II) ions. Every Eu_2 C8A SUB bridges two Co(II) ions
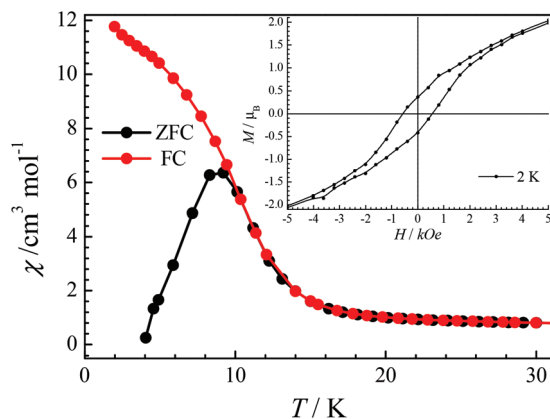

Fig. 6 Temperature dependence of the in-phase (χ') and out-of-phase (χ'') ac susceptibility signals under a zero dc field at the indicated frequencies for **CIAC-249**.

(Co_2 dimer), and three Co_2 dimers result in a triangular structure. Such a triangular geometry often leads to spin frustration with spin-glass ground state.

The magnetic dynamics for **CIAC-250** was studied using ac magnetic susceptibility measurements under a zero dc field. As shown in Fig. 7, χ' signals diverge at nearly 30 K without reaching the maximum (except for high frequencies) and splitting tails of χ'' signals were observed above 2 K, indicating the slow relaxation of magnetization, a characteristic SMM behaviour, but with the existence of fast quantum tunneling of magnetization (QTM). The parameter φ is calculated as 0.51, which is larger than the value for a spin glass, but close to a superparamagnetic behaviour. The relaxation times (τ) at different temperatures for **CIAC-250** are evaluated from variable-frequency data via a generalized Debye model (Fig. S11 and S12†).[39] The obtained $\ln(\tau)$ values remain linear between 5.4 and 3.5 K, showing a thermally activated process, which can be fitted by the Arrhenius law, giving U_{eff} = 41.5 K and τ_0 = 8.50 ×

Fig. 5 χ–T plots of **CIAC-249** under field-cooled (FC) and zero-field-cooled (ZFC) conditions with a field of 50 Oe. Inset: Field-dependent magnetizations for complex **CIAC-249** from 0 to 50 kOe at 2 K.
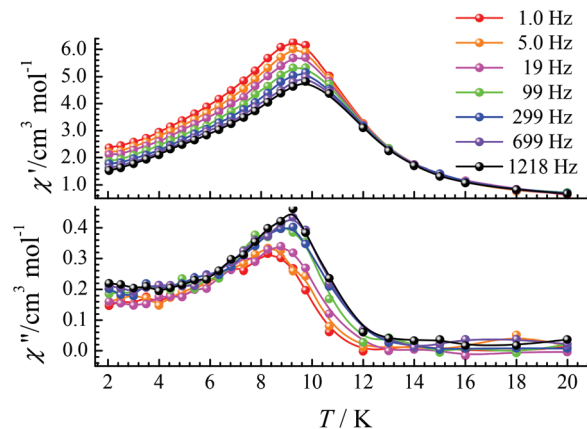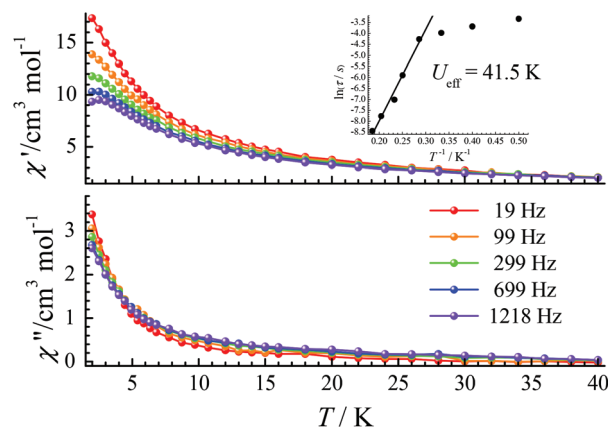

Fig. 7 Temperature dependence of the in-phase (χ') and out-of-phase (χ'') ac susceptibility signals under a zero dc field at the indicated frequencies for **CIAC-250**. The lines are visual guides only. Inset: Plots of ln (τ) versus 1/T for **CIAC-250**. The solid line is the best fit.
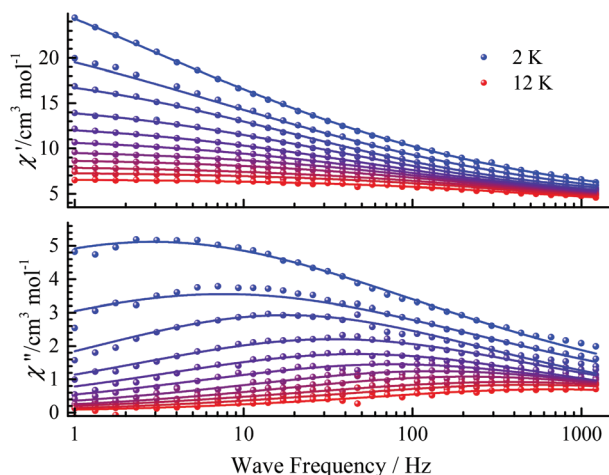
Fig. 8 Frequency dependence of χ' and χ'' ac susceptibility signals under a 500 Oe dc field at the indicated temperatures for **CIAC-250**. The solid lines are the best fits.

10^{-8} s (inset in Fig. 7). A slight deviation occurs as the temperature further decreases, which could be attributed to strong QTM at low temperature.

To suppress the QTM, ac magnetic susceptibilities were measured under a dc field of 500 Oe from 2 K to 12 K (Fig. 8), which was fitted with a generalized Debye model (Fig. 9).[35] The α parameters range from 0.50 to 0.64, indicating a wide contribution for the relaxation times. The obtained $\ln(\tau)$ values remain linear above 6 K and with slight curvatures at low temperature, but do not become temperature independent. The linear regime at high temperature is often known as the Orbach relaxation process, while for low temperature it can be regarded as the Raman relaxation process because it is not temperature independent. So the Orbach process was combined with the Raman process to fit the relaxation times, giving $C = 3.0(5)$ s^{-1} K^n, $n = 2.6(1)$, $\tau_0 = 3(2) \times 10^{-6}$ s and $U_{\text{eff}} = 56(9)$ K (Fig. 9).
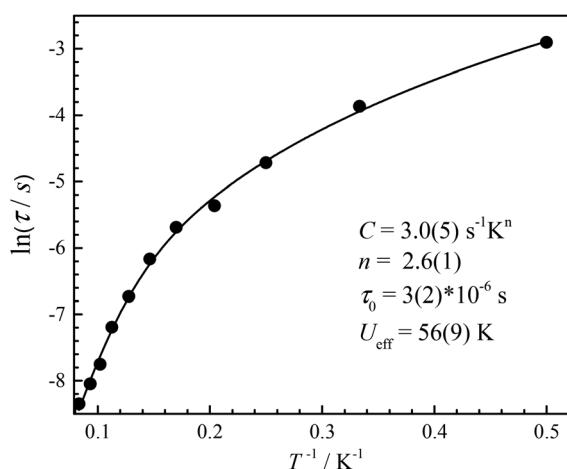

Fig. 9 Plots of $\ln(\tau)$ versus $1/T$ for **CIAC-250** under a 500 Oe dc field. The solid line is the best fit.

Conclusions

In conclusion, we have synthesized $\{(Ln_6^{III}Co_6^{II})(C8A)_3\}$ clusters featuring a wrapped $[Co_6]$ hexagon linked to three calix[8]arene molecules in a double-cone conformation. Interestingly, the $\{Eu_6Co_6\}$ cluster shows spin glass behaviours below ≈ 9 K, while the $\{Dy_6Co_6\}$ cluster exhibits SMM behaviour with U_{eff} of 41.5 K under a zero dc field (56(9) K under a 500 Oe dc field). This result emphasized that larger calix[n]arene ($n = 6, 7, 8$) with more coordination sites and larger molecules will provide further opportunities for controlling the self-assembly and tuning of the magnetic properties. Exploration of another transition metal, Ln, and mixed transition-metal/Ln clusters supported by methylene-bridged calix[8]arenes is underway to generate other novel functional materials.

Conflicts of interest

There are no conflicts to declare.

Acknowledgements

Notes and references

1 L. R. Piquer, S. Dey, L. C. Amorós, S. J. Teat, J. Cirera, G. Rajaraman and E. C. Sañudo, Microwave assisted synthesis of heterometallic 3d–4f M$_4$L$_n$ complexes, *Dalton Trans.*, 2019, **48**, 12440.

2 V. Das, R. Kaushik and F. Hussain, Heterometallic 3d-4f polyoxometalates: An emerging field with structural diversity to multiple applications, *Coord. Chem. Rev.*, 2020, **143**, 213271.

3 J. Wang, M. Feng, M. N. Akhtar and M. L. Tong, Recent advance in heterometallic nanomagnets based on TM$_x$Ln$_{4-x}$ cubane subunits, *Coord. Chem. Rev.*, 2019, **387**, 129.

4 G. Karotsis, S. J. Teat, W. Wernsdorfer, S. Piligkos, S. J. Dalgarno and E. K. Brechin, Calix[4]arene-Based Single-Molecule Magnets, *Angew. Chem., Int. Ed.*, 2009, **48**, 8285.

5 G. Karotsis, S. Kennedy, S. J. Teat, C. M. Beavers, D. A. Fowler, J. J. Morales, M. Evangelisti, S. J. Dalgarno and E. K. Brechin, [Mn$^{III}_4$Ln$^{III}_4$] calix[4]arene clusters as enhanced magnetic coolers and molecular magnets, *J. Am. Chem. Soc.*, 2010, **132**, 12983.

6 G. Karotsis, M. Evangelisti, S. J. Dalgarno and E. K. Brechin, A calix[4]arene 3d/4f magnetic cooler, *Angew. Chem., Int. Ed.*, 2009, **48**, 9928.

7 S. M. Taylor, G. Karotsis, R. D. McIntosh, S. Kennedy, S. J. Teat, C. M. Beavers, W. Wernsdorfer, S. Piligkos, S. J. Dalgarno and E. K. Brechin, A family of calix[4]arene-supported [$Mn^{III}_2Mn^{II}_2$] clusters, *Chem. – Eur. J.*, 2011, **17**, 7521.

8 Y. F. Bi, X. T. Wang, B. W. Wang, W. P. Liao, X. F. Wang, H. J. Zhang, S. Gao and D. Q. Li, Two $Mn^{II}_2Ln^{III}_4$ (Ln=Gd, Eu) hexanuclear compounds of *p-tert*-butylsulfinylcalix[4]arene, *Dalton Trans.*, 2009, 2250.

9 Y. F. Bi, Y. L. Li, W. P. Liao, H. J. Zhang and D. Q. Li, A unique Mn_2Gd_2 tetranuclear compound of *p-tert*-butylthiacalix[4]arene, *Inorg. Chem.*, 2008, **47**, 9733.

10 C. M. Liu, D. Q. Zhang, X. Hao and D. B. Zhu, Syntheses, crystal structures, and magnetic properties of two *p-tert*-butylsulfonylcalix[4]arene-supported cluster complexes with a totally disordered $Ln_4(OH)_4$ cubane core, *Cryst. Growth Des.*, 2012, **12**, 2948.

11 R. Zairov, S. Pizzanelli, A. P. Dovzhenko, I. Nizameev, A. Orekhov, N. Arkharova, S. N. Podyachev and S. Sudakova, Paramagnetic relaxation enhancement in hydrophilic colloids based on Gd(III) complexes with tetrathia-and calix[4]arenes, *J. Phys. Chem.*, 2020, **124**(7), 4320.

12 J. Y. Ge, X. Duan, J. P. Ma, S. Huang, J. Du and P. Wang, Thiacalix[4]arene-supported tetranuclear Tb^{III} and Eu^{III} compounds: Synthesis, structure, luminescence, and magnetism, *Z. Anorg. Allg. Chem.*, 2019, **645**, 416.

13 R. O. Fuller, G. A. Koutsantonis and M. I. Ogden, Magnetic properties of calixarene-supported metal coordination clusters, *Coord. Chem. Rev.*, 2020, **402**, 213066.

14 R. McLellan, S. M. Taylor, R. D. McIntosh, E. K. Brechin and S. J. Dalgarno, Complementary ligands direct the formation of a calix[8]arene-supported ferromagnetic $Mn^{IV}Mn^{III}$ dimer, *Dalton Trans.*, 2013, **42**, 6697.

15 S. M. Taylor, S. Sanz, R. D. McIntosh, C. M. Beavers, S. J. Teat, E. K. Brechin and S. J. Dalgarno, *p-tert*-Butylcalix[8]arene: An extremely versatile platform for cluster formation, *Chem. – Eur. J.*, 2012, **18**, 16014.

16 H. S. Wang, Y. Chen, Z. B. Hu, Q. Q. Long, C. L. Yin, Z. C. Zhang and Z. Q. Pan, A Dy-based complex with the magnetic relaxation behavior regulated by enclosing one Dy^{III} ion into a Calix[8]arene ligand, *Inorg. Chem. Commun.*, 2019, **105**, 76.

17 H. T. Han, X. L. Li, X. F. Zhu, G. S. Zhang, S. T. Wang, X. X. Hang, J. K. Tang and W. P. Liao, Single-molecule magnet behavior in a calix[8]arene-capped {$Tb_6^{III}Cr^{III}$} cluster, *Eur. J. Inorg. Chem.*, 2017, **14**, 2088.

18 H. T. Han, X. L. Li, X. F. Zhu, G. S. Zhang, X. X. Hang, J. K. Tang and W. P. Liao, Single molecule magnet behavior in a calix[8]arene-capped heterometallic {$Dy^{III}_4Co^{II}_4$} square antiprismatic cluster, *Eur. J. Inorg. Chem.*, 2017, **41**, 4879.

19 S. Haldara, G. Vijaykumar, L. Carrella, G. T. Musie and M. Bera, Structure and properties of a novel staircase-like decanuclear [Cu^{II}_{10}] cluster supported by carbonate and carboxylate bridges, *New J. Chem.*, 2018, **42**, 1276.

20 K. S. Brzostek, M. Terlecki, K. Sokołowski and J. Lewiński, Chemical fixation and conversion of CO_2 into cyclic and cage-type metal carbonates, *Coord. Chem. Rev.*, 2017, **334**, 199.

21 B. Das, M. Bhadbhade, A. Thapper, C. D. Ling and S. B. Colbran, A new trinuclear Cu-carbonate cluster utilizing CO_2 as a C1-building block -reactive intermediates, a probable mechanism, and EPR and magnetic studies, *Dalton Trans.*, 2019, **48**, 3576.

22 W. Meng, H. F. Ye, S. Liu, F. Xu and W. J. Xu, Emergence of complex chiral coordination clusters {$Cu^{II}_{48}Na_{12}$} by using multiple ligands under oxidizing conditions, *Dalton Trans.*, 2019, **48**, 3204.

23 E. Guarda, K. Bader, J. V. Slagerenb and P. Alborés, {$Ni^{II}_8Ln^{III}_6$} (Ln=Gd, Dy) rod-like nano-sized heteronuclear coordination clusters with a double carbonate bridge skeleton and remarkable MCE behaviour, *Dalton Trans.*, 2016, **45**, 8566.

24 H. Q. Tian, L. Zhao and J. K. Tang, Exploiting miraculous atmospheric CO_2 fixation in the design of dysprosium single-molecule magnets, *Cryst. Growth Des.*, 2018, **18**, 1173.

25 X. M. Zhang, P. Li, W. Gao, J. P. Liu and E. Q. Gao, A new cube-based dodecanuclear cobalt(II) cluster with azide and tetrazolate ligands exhibiting ferromagnetic ordering, *Dalton Trans.*, 2015, **44**, 13581.

26 S. Schmitz, J. V. Leusen, A. Ellern, P. Kögerler and K. Y. Monakhov, Thioether-terminated nickel(II) coordination clusters with {Ni_6} horseshoe-and {Ni_8} rollercoaster-shaped cores, *Inorg. Chem. Front.*, 2016, **3**, 523.

27 G. J. Cooper, G. N. Newton, P. Kögerler, D. L. Long, L. Engelhardt, M. Luban and L. Cronin, Structural and compositional control in {M_{12}} cobalt and nickel coordination clusters detected magnetochemically and with cryospray mass spectrometer, *Angew. Chem., Int. Ed.*, 2007, **46**, 1340.

28 C. D. Gutsche, B. Dhawan, K. H. No and R. Muthukrishnan, Calixarenes. 4. The synthesis, characterization, and properties of the calixarenes from p-tert-butyl-phenol, *J. Am. Chem. Soc.*, 1981, **103**, 3782.

29 G. M. Sheldrick, *SHELXS-97, A computer program for the solution of crystal structures, PC version*, University of Göttingen, Göttingen, Germany, 1997.

30 D. Casanova, P. Alemany, J. M. Bofill and S. Alvarez, Shape and symmetry of hepta coordinate transition-metal complexes: structural trends, *Chem. – Eur. J.*, 2003, **9**, 1281.

31 D. Casanova, M. Llunell, P. Alemany and S. Alvarez, The rich stereochemistry of eight-vertex polyhedra: a continuous shape measures study, *Chem. – Eur. J.*, 2005, **11**, 1479.

32 Y. H. Wan, L. P. Zhang, L. P. Jin, S. Gao and S. Z. Lu, High-dimensional architectures from the self-assembly of lanthanide ions with benzenedicarboxylates and 1,10-phenanthroline, *Inorg. Chem.*, 2003, **42**, 4985.

33 N. F. Chilton, R. P. Anderson, L. D. Turner, A. Soncini and K. S. Murray, PHI: A powerful new program for the analysis of anisotropic monomeric and exchange-coupled poly-nuclear d- and f-block complexes, *J. Comput. Chem.*, 2013, **34**, 1164.

34 N. A. Chernova, Y. N. Song, P. Y. Zavalij and M. S. Whittingham, Solitary excitations and domain-wall

This journal is © the Partner Organisations 2020

Inorg. Chem. Front., 2020, **7**, 4070–4076 | **4075**

movement in the two-dimensional canted antiferromagnet $(C_2N_2H_{10})_{1/2}FePO_4(OH)$, *Phys. Rev. B: Condens. Matter Mater. Phys.*, 2004, **70**, 144405.

35 J. A. Mydosh, *Spin Glasses: An Experimental Introduction*, Taylor & Francis, London, 1993.

36 M. A. Novak, Magnetic relaxation in molecular nano-structures, *J. Magn. Magn. Mater.*, 2004, **272–276**, E707.

37 Y. Z. Yu, Y. H. Guo, Y. R. Zhang, X. J. Tian and X. M. Zhang, Tetrahedral μ_4-chloride and in situ generated octahedral μ_6- sulfide templating Co_8 complexes with different distortions of the cube, *Chem. Commun.*, 2020, **56**, 4236–4239.

38 Q. Chen, M. H. Zeng, L. Q. Wei and M. Kurmoo, A multi-faceted cage cluster, $[Co^{II}_6O_{12} \supset X]^-$ (X=Cl$^-$ or F$^-$): Halide template effect and frustrated magnetism, *Chem. Mater.*, 2010, **22**, 4328.

39 Y. N. Guo, G. F. Xu, Y. Guo and J. K. Tang, Relaxation dynamics of dysprosium(III) single molecule magnets, *Dalton Trans.*, 2011, **40**, 9953.